Sturtevant, J. M. S. A., & Geiduschek, E. P. (1958) *Discuss. Faraday Soc. 25*, 138–148.
Wilson, W. D., Krishnamoorthy, C. R., Wang, Y.-H., & Smith, J. C. (1985) *Biopolymers 24*, 1941–1961.
Zimmer, Ch., & Venner, H. (1966) *Biopolymers 4*, 1073–1079.
Zimmer, Ch., Luck, G., & Venner, H. (1968) *Biopolymers 6*, 563–574.

Nuclease Activity of 1,10-Phenanthroline–Copper Ion: Reaction with CGCGAATTCGCG and Its Complexes with Netropsin and *Eco*RI†

Michio Kuwabara, Chun Yoon, Thomas Goyne, Theodore Thederahn, and David S. Sigman*

Department of Biological Chemistry, School of Medicine, and Molecular Biology Institute, University of California, Los Angeles, California 90024

Received March 24, 1986; Revised Manuscript Received July 22, 1986

ABSTRACT: The self-complementing dodecamer 5′-CGCGAATTCGCG-3′ and its complexes with the antibiotic netropsin and the restriction endonuclease *Eco*RI provide substrates of known three-dimensional structure to study the stereochemistry and mechanism of the artificial nuclease of 1,10-phenanthroline–copper ion [$(OP)_2Cu^+$]. Analysis of the reaction products with the 5′-^{32}P dodecamer on 20% sequencing gels has demonstrated the presence of 3′-phosphoglycolate ends in addition to 3′-phosphomonoester ends expected from previous studies. A reaction intermediate, which is a precursor to 3′-phosphomonoester termini, has been trapped; in contrast, no comparable species for the 5′-phosphomonoester termini can be detected when 3′-labeled DNAs are utilized as substrates. The reactive oxidative species formed by the coreactants $(OP)_2Cu^+$ and hydrogen peroxide is distinguishable in its chemistry from the hydroxyl radicals produced by cobalt-60 γ-irradiation. The freely diffusible hydroxyl radicals generated by cobalt-60 irradiation produce equivalent amounts of 3′-phosphomonoester and 3′-phosphoglycolate termini whereas the 3′-phosphomonoesters are the preferred product of $(OP)_2Cu^+$ and H_2O_2. On the basis of the structures of the products obtained, the principal site of attack of the coordination complex is on the C-1 of the deoxyribose within the minor groove. This conclusion is supported by the footprinting of netropsin binding to the dodecamer. Crystallographic results have demonstrated that netropsin binds to the minor groove at the central AATT residue. A clear protection of attack by the coordination complex at the deoxyriboses associated with A-5, T-6, T-7, and C-9 is fully consistent with attack from the minor groove without intercalation during the course of the cleavage reaction. *Eco*RI binds to the tridecamer TCGCGAATTCGCG by interactions in the major groove, leaving the minor groove accessible to solvent. Consistent with the proposed attack of $(OP)_2Cu^+$ in the minor groove, the restriction endonuclease does not protect the dodecamer from oxidative attack.

The 1,10-phenanthroline–cuprous complex[1] with hydrogen peroxide as a coreactant is an artificial nuclease that cleaves DNA by an oxidative mechanism under physiological conditions (Sigman et al., 1979). $(OP)_2Cu^+$ preferentially cleaves B-form DNA over A DNA; it does not cleave the left-handed Z structure or single-stranded DNA incapable of forming secondary structures (Marshall et al., 1981; Pope & Sigman, 1984). The conformational sensitivity of the nuclease action probably results from the obligatory formation of a noncovalent intermediate between the coordination complex and the DNA during the course of the reaction.

Recent studies using restriction fragments containing the *lac* control region as substrates have clearly demonstrated that $(OP)_2Cu^+$ reactivity depends upon primary sequence but that all bases (e.g., A, T, G, and C) may serve as hypersensitive sites (Sigman et al., 1985; Spassky & Sigman, 1985). The conserved promoter sequence (Pribnow, 1975) represents one region of preferential cutting. Single base changes in this region cause dramatic alterations in the cleavage pattern, reflecting the sensitivity of the nuclease activity to the primary sequence but not to a single base. For example, $(OP)_2Cu^+$ cleaves the 5′-labeled template strand of the control region of the wild-type promoter strongly at residues cytosine-13 and adenine-12. In the $(OP)_2Cu^+$ cleavage of the template strand isolated from the Ps variant, which differs from the wild-type by a single base change at residue C-9 (cytosine to thymidine), an additional hypersensitive band becomes apparent at adenine-10 (Sigman et al., 1985). Enhanced reactivity to the reagent implies that the single base change alters the local conformation of the DNA to provide a more productive binding site for the coordination complex.

In order to identify those features of DNA conformation that enhance its reactivity to the reagent, we studied the reactivity of the coordination complex with a B DNA of known three-dimensional structure, the self-complementing dode-

† This research was supported by USPHS (21199) and by the American Cancer Society (BC 410). T.G. and T.T. were supported by Grant 5T32 CA 9030 awarded by the National Cancer Institute.

* Address correspondence to this author.

[1] Abbreviations: OP, 1,10-phenanthroline; $(OP)_2Cu^+$, 2:1 1,10-phenanthroline–cuprous ion complex; $(OP)_2Cu^{2+}$, 2:1 1,10-phenanthroline–cupric ion complex; MPA, 3-mercaptopropionic acid; Tris,tris(hydroxymethyl)aminomethane; EDTA, ethylenediaminetetraacetic acid.

0006-2960/86/0425-7401$01.50/0

camer CGCGAATTCGCG (Drew & Dickerson, 1981a,b; Dickerson & Drew, 1981a,b; Fratini et al., 1982; Dickerson et al., 1982). The digestion of this double-stranded oligonucleotide by DNase I has been previously carried out in order to identify the structural preferences of the enzyme (Lomonosoff et al., 1981).

In this paper, we present evidence that the coordination complex cleaves DNA by attacking the deoxyribose from the minor groove. Analysis of the reaction products and footprinting studies using dodecamer–netropsin and dodecamer–*Eco*RI complexes, both structures that have been solved by X-ray crystallographic methods (Kopka et al., 1985a,b; Frederick et al., 1984), provides strong support for this conclusion. However, no single structural parameter (e.g., base roll, propellor twist, or helical twist angle) has been identified that can account for the preferred cutting by $(OP)_2Cu^+$. During the course of these studies, we have trapped an intermediate formed during the reaction that converts to 3′-phosphorylated ends upon standing at −20 °C or incubation with 1 M piperidine.

Experimental Procedures

Materials

The dodecamer CGCGAATTCGCG and netropsin were a gift of Professor R. E. Dickerson and Dr. Mary Kopka. Professor John Rosenberg kindly provided a sample of magnesium ion free *Eco*RI. The following chemicals were obtained from commercial sources and used without further purification: 1,10-phenanthroline and 2,9-dimethyl-1,10-phenanthroline (G. F. Smith); 3-mercaptopropionic acid (Aldrich); T-4 polynucleotide kinase (BRL); spermidine, dithiothreitol, Tris, and DNase I (Sigma); acrylamide, bis(acrylamide) (Bio-Rad); [γ-^{32}P]ATP (ICN); magnesium chloride, EDTA, and copper sulfate (Mallinckrodt).

Methods

Labeling of Dodecamer. The dodecamer was labeled at the 5′-end with [γ-^{32}P]ATP under the reaction conditions described in Maniatis et al. (1982). The oligonucleotides were purified from excess [γ^{32}P]ATP by acetonitrile step elution from a C-18 column. When necessary, oligonucleotides may be further purified on 20% denaturing acrylamide gels, eluting with a buffer composed of 0.5 M ammonium acetate and 1 mM EDTA at pH 8.0. Duplexes were formed by heating the oligonucleotide in buffer at 90 °C for 5 min followed by cooling at room temperature for 1 h. The dodecamer was stored as the duplex at −20 °C.

$(OP)_2Cu^+$ Digestion. The digestion of the dodecamer by $(OP)_2Cu^+$ was carried out in 50 mM Tris-HCl pH 8.0 buffer, 170 μM OP, 40 μM $CuSO_4$, and 4.8 mM 3-mercaptopropionic acid with 5×10^6 cpm of the dodecamer and quenched at the desired time points by addition of 2,9-dimethyl-OP to 2 mM and cooling to 0 °C. Evaporation of the reaction mixture to dryness and redissolving in loading buffer traps the metastable intermediary products. These reaction products remain stable for at least 1 day at −20 °C in the loading buffer. Alternatively, heating the metastable species to 90 °C after the drying step in a solution made 1.0 M in piperidine for 30 min transforms the products to oligonucleotides with 3′-phosphomonoester termini. If the metastable species are stored frozen after the addition of the 2,9-dimethyl-OP for 3 days, dried, and then dissolved in loading buffer, the intermediates are converted to the 3′-phosphomonoester.

In the footprinting experiments with netropsin and *Eco*RI, reaction mixtures were quenched with 2,9-dimethyl-1,10-phenanthroline, evaporated to dryness, heated with 100 μL of 1.0 M piperidine for 30 min at 90 °C, dried, washed with water, and dried again. The resulting products were then dissolved in a loading buffer and electrophoresed on a 20% sequencing gel. Electrophoresis was carried out as previously described (Maxam & Gilbert, 1980). Exposure times were adjusted to allow visualization of relevant bands. Gels were developed in a Pako automatic film developer.

For the dodecamer, incubation with piperidine generates a background of 5′-labeled oligonucleotides (lane b) that are not present in the labeled oligonucleotide alone. The background bands arise either from the removal of bases during the course of chemical synthesis or, more likely, from the radiation-induced damage by ^{32}P of the labeled terminus, which causes piperidine sensitivity and is more readily visualized in a short oligonucleotide. The latter explanation is favored by the following observation. If the band corresponding to the dodecamer is eluted from a sequencing gel after treatment with piperidine, retreated with piperidine, and subjected to electrophoresis again under identical conditions, the same pattern of products appears (cf. Figure 1).

Nuclease and Cobalt-60 Scission. A total of 1×10^6 cpm of 5′-labeled dodecamer was digested with 500 units/mL of either DNase I or *Eco*RI in 50 mM Tris-HCl at pH 7.5, 5 mM $MgCl_2$, 50 mM NaCl, and 1 mM dithiothreitol at 37 °C. Both enzymatic digestions were quenched by bringing the digestions to 15% sucrose (w/v), 7 M urea, 10 mM EDTA, and 0.1% bromophenol blue and added directly to the 20% sequencing gel. For ^{60}Co irradiation, 1×10^6 cpm of labeled oligonucleotide was exposed to 10000 rad with an AES Gamma Cell 220 ^{60}Co source (1193 rad/min) in distilled water under aerobic conditions. The reaction products then were evaporated to dryness and redissolved in the loading buffer of the sequencing gels.

Kinetic Analysis. Densitometric methods were used to analyze sequencing gels. To ensure that the density of bands in the autoradiograph of the gels lies in the linear response portion of the X-ray film (Kodak XAR), a sequencing gel was loaded with a serial dilution of the cleaved dodecamer. An autoradiograph of the gel was analyzed by densitometry to show that the band densities increased linearly with concentration. Subsequent gels used in this analysis were loaded with oligonucleotide such that the concentration of the cleaved fragments was within this range.

Microdensitometry of autoradiographs was performed on an P-1000 drum scanner (Optronics International, Inc) driven by a VAX 11/780 (Digital Equipment Corp.). All gel lanes were scanned in 0.1-mm increments. To facilitate the sequence assignment of each band, DNA samples subjected to Maxam–Gilbert A+G sequencing procedures were loaded in neighboring lanes. Bands that overlapped in the autoradiograph were resolved by using Gaussian-distributed approximations to the individual band densities. Since the concentration was directly proportional to the measured density, the total density of each lane was scaled to the value measured for the control lane (no cleavage) to normalize for the amount of labeled DNA in each gel lane.

By limiting DNA digestion to very brief times, one can approximate the oxidative cleavage of DNA with pseudo-first-order kinetics. Comparison of cleavage rate constants from the reaction of $(OP)_2Cu^+$ with the labeled dodecamer for different durations verified that the calculated first-order rate constants are unchanged for reaction times up to 1 min. A reaction that proceeds with first-order kinetics permits the straightforward calculation of cleavage rate constants according to an algorithm that does not require the assumption

that $(OP)_2Cu^+$ cleaves each oligonucleotide only once. The method calculates rate constants after incorporating the probability of cleavage at all sites closer to the 5′-labeled end.

An additional observation is important in discussing the kinetics of the chemical nuclease. The pseudo-first-order rate constants calculated as described above decrease as a function of time of incubation. This can be attributed to the consumption of reactants free in solution during the reaction interval. The utilization of thiol and the destruction of the phenanthroline by the oxidative intermediates produced by the $(OP)_2Cu^+$ complex, in the presence of the reducing agent and oxygen, result in the observed decrease in the calculated first-order rate constants. The oxidative chemistry occurring free in solution does not lead to DNA strand scission because of the efficient quenching of hydroxyl radicals by the Tris buffer and other components of the reaction mixture including 1,10-phenanthroline.

Results

Product Analysis. The products of the $(OP)_2Cu^+$ cleavage of poly(dA-T) include the free bases adenine and thymine and phosphomonoesters at the 3′- and 5′-termini (Marshall et al., 1981; Pope & Sigman, 1984). Studies with a 186 base pair restriction fragment of the *lac* operon confirmed the formation of 3′- and 5′-phosphomonoesters by calibrating sequencing gel digests of $(OP)_2Cu^+$ with products of the Maxam–Gilbert G+A chemical sequencing reactions (Sigman et al., 1985; Spassky & Sigman, 1985). In studies with the 186 base pair restriction fragment, ethanol precipitation, sometimes after phenol extraction, was used to prepare the cleavage products for analysis by electrophoresis (Sigman et al., 1985; Spassky & Sigman, 1985).

Kinetic analysis of the scission of the dodecamer required a measure of all the different products formed during the oxidation of the DNA by the coordination complex. Because of the possible variability in recovery of the short products arising from the scission of the dodecamer, the protocol for sample preparation was altered in two ways. Ethanol precipitation was avoided during the preparation of fragments for electrophoretic analysis. Instead, reaction mixtures containing the cleaved dodecamer were dried immediately after quenching with 2,9-dimethyl-1,10-phenanthroline, then dissolved in loading buffer, and applied to the gel. As noted below, small changes in the method of solvent preparation after quenching with 2,9-dimethyl-1,10-phenanthroline permitted the isolation of an intermediate. Second, the analysis of the digestion pattern of the 5′-labeled dodecamer required the resolution provided by a 20% sequencing gel. The 5′-labeled dodecamer was cleaved by four different methods to provide a complete set of standards of possible products. These included the Maxam–Gilbert G+A cleavage reactions, which yield 3′-phosphate (Maxam & Gilbert, 1980), ^{60}Co irradiation, which generates 3′-phosphomonoesters and 3′-phosphoglycolates (Henner et al., 1982, 1983), and DNase I and *Eco*RI, which leave 3′-hydroxyl groups on the ends of DNA fragments.

The electrophoretic results presented in Figure 1 yield important insights into the chemistry of the DNA strand scission by $(OP)_2Cu^+$. The products of cobalt-60 irradiation (Figure 1, lane c) are 3′-phosphorylated termini and the faster migrating 3′-phosphoglycolate. Both are produced in equivalent amounts at each position in the sequence. 3′-Phosphorylated products at each position in the sequence can also be detected if the labeled dodecamer is simply heated in the presence of 1 M piperidine (Figure 1, lane b). This base lability may be reflective either of radiation-induced damage from the 5′-^{32}P

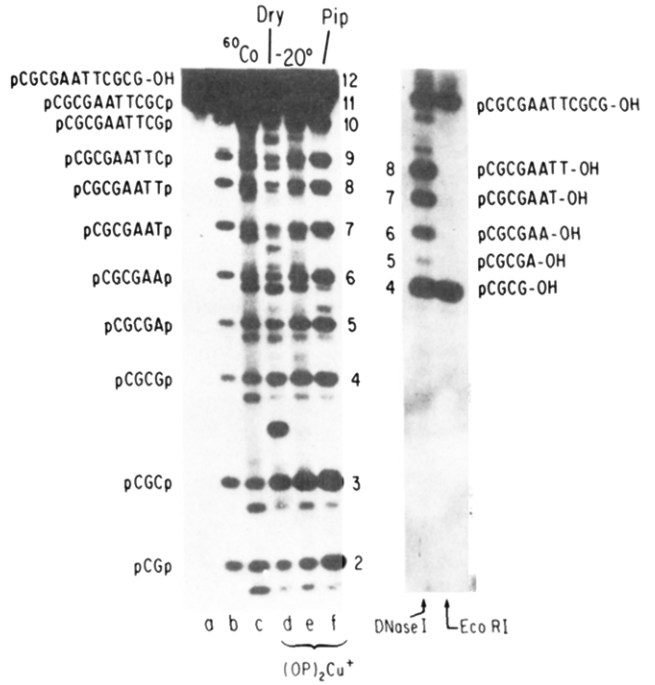

FIGURE 1: Scission of dodecamer by $(OP)_2Cu^+$, DNase I, cobalt-60, and *Eco*RI. Conditions of cleavage are summarized under Experimental Procedures: (a) control; (b) dodecamer heated with piperidine; (c) cobalt-60 irradiated; (d–f) $(OP)_2Cu^+$ but treated differently subsequent to quenching [(d) dried immediately; (e) frozen and stored for 3 days and then dried and dissolved in loading buffer; (f) dried immediately and then heated with 1 M piperidine. Maxam–Gilbert sequencing lanes are not shown.

label or of the loss of base during the chemical synthesis of the oligonucleotide. Since both DNase I and *Eco*RI produce nucleotides with a free 3′-hydroxyl group, the failure of any product of the $(OP)_2Cu^+$ cleavage reaction to comigrate with the hydrolysis products of these enzymes indicates that the artificial nuclease does not generate them. The product distribution in DNase I digests closely corresponds to those presented by Lomonosoff et al. (1981), who used thin-layer chromatography to analyze the products.

Hydrolysis by *Eco*RI provides important confirmation that the dodecamer has formed the duplex under our experimental conditions of 4.4 μM of the single-stranded oligonucleotide and 37 °C. The formation of double-stranded dodecamer is consistent with nuclear magnetic resonance studies of the melting transition of the double-stranded dodecamer. These experiments have demonstrated a common midpoint for the nonexchangeable hydrogens for the dG-dC base pairs at positions 2, 3, and 4 and dA-dT base pairs at positions 5 and 6 of 72 ± 2 °C in 0.1 M phosphate buffer (Patel et al., 1982).

Trapping of a Metastable Intermediate. Unexpectedly, the electrophoretic patterns for $(OP)_2Cu^+$ proved dependent on the conditions of the preparation of the sample prior to dissolving in loading buffer. These observations led to the discovery of a metastable intermediate. Drying the samples immediately following the quenching with 2,9-dimethyl-1,10-phenanthroline and then dissolving in loading buffer produced the digestion pattern seen in Figure 1, lane d. In contrast, storing the sample at −20 °C for 3 days before evaporating to dryness and dissolving in loading buffer yields the pattern seen in Figure 1, lane e. The most obvious difference between these lanes is the strong band running between the trimer and tetramer in lane d but not observed in lane e. It migrates differently from the 3′-monophosphoesters and 3′-glycolates that have been generated by γ-irradiation (lane c, Figure 1) (Henner et al., 1982, 1983) and from the 3′-

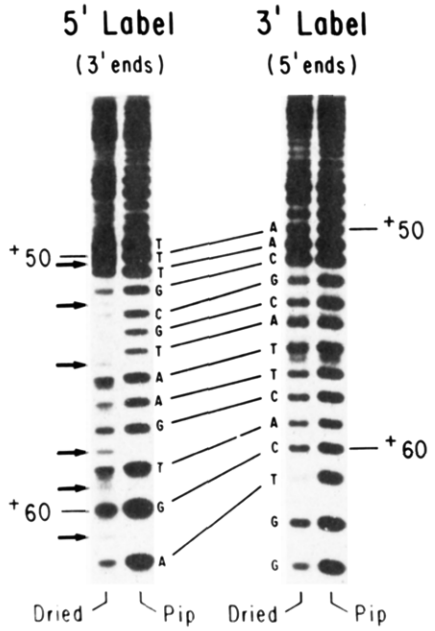

FIGURE 2: Comparison of cleavage patterns of 5′- and 3′-labeled DNAs. Uniquelly labeled 187 base pair fragments encompassing the *lac* control region were prepared from a 203 *Eco*RI fragment followed by secondary *Pvu*II restriction: 5′-labeled DNA (template strand) initially phosphorylated with polynucleotide kinase and 3′-labeled DNA by end filling with Klenow fragment and [^{32}P]dATP. Digests with $(OP)_2Cu^+$ were quenched with 2,9-dimethyl-1,10-phenanthroline and then dried (Dried) or dried and then heated with 1 M piperidine (Pip) prior to electrophoresis. Arrows indicate metastable peaks in 5′-labeled products. In the original autoradiograph, faint bands are apparent in the "dried" 5′ label gel at positions 53–55 and in the "dried" 3′ label gel at position 61.

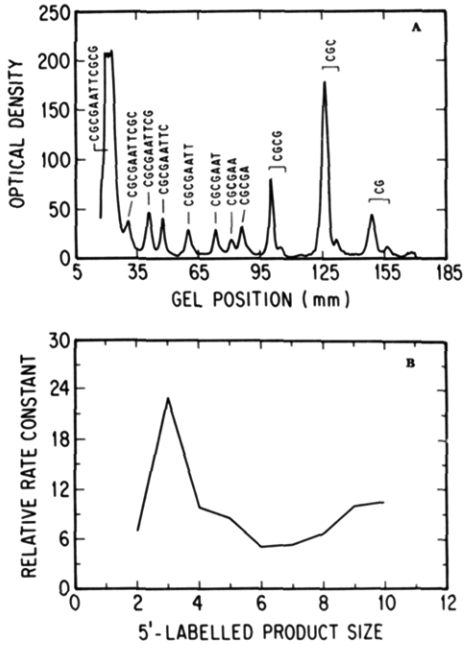

FIGURE 3: Quantitation by densitometry: (A) densitometer trace of lane f, Figure 1; (B) calculation of relative first-order rate constants.

hydroxyl derivatives produced by DNase I digestion of the same oligonucleotide. In addition to their gradual conversion to the 3′-phosphorylated products upon standing at −20 °C, heating the reaction products to 90 °C for 0.5 h in 1 M piperidine efficiently transforms the product in this band to the 3′-phosphomonoester (lane f).

3-Phosphoglycolate Termini. Base treatment with 1 M piperidine also converts 3′-phosphoglycolates to 3′-phosphomonoesters. Lanes c and d of Figure 1 compare the yield of 3′-phosphoglycolate products formed by irradiation and $(OP)_2Cu^+$ without piperidine treatment prior to electrophoresis. Two important differences are observed in the production of the phosphoglycolates. First, ^{60}Co irradiation produces approximately equivalent amounts of 3′-phosphoglycolates and 3′-phosphomonoesters. In contrast, the amount of 3′-phosphoglycolate in the $(OP)_2Cu^+$-mediated cleavage usually is substantially less than that of the 3′-phosphomonoester. Second, the yield of the phosphoglycolate by hydroxyl radicals generated by ^{60}Co is independent of sequence. For $(OP)_2Cu^+$, the relative yield of the two products depends on sequence.

Absence of 5′ Metastable Products. The discovery of a metastable product on the 3′-end of the dodecamer prompted us to investigate if a comparable product forms on the 5′-end. However, 3′-labeled dodecamer, essential for observing products at the 5′-terminus, is not readily prepared. In order to examine products at the 5′-end, a 3′-labeled restriction fragment containing the lactose (*lac*) control region was used as substrate (Spassky & Sigman, 1985). $(OP)_2Cu^+$ cleavage of the same fragment labeled at the 5′-end verified that the metastable products at the 3′-end were not unique to the dodecamer. As in the case of the dodecamer, analysis of the digests of the 5′-labeled substrates revealed metastable species indicative of 3′-ends bearing remnants of the deoxyribose (Figure 2). Heating these intermediates with 1 M piperidine or storage at −20 °C before drying resulted in their conversion into 3′-phosphomonoesters. The 3′-labeled derivatives did not demonstrate any unusual or unstable products after the reaction mixture was evaporated to dryness. Storage at −20 °C or incubation with piperidine did not alter the products, which moved at the same rate as the 5′-phosphomonoester products of the Maxam–Gilbert cleavage reaction on a sequencing gel (Figure 2). The absence of 5′-transient products with the *lac* fragment would render unlikely the occurrence of such products in the dodecamer.

Kinetic Analysis of Cleavage of Dodecamer. The relative rates of formation of all products from the $(OP)_2Cu^+$ cleavage of the 5′-labeled dodecamer were determined from densitometry data. A representative example of a densitometry trace and the calculated relative rate constants for the cleavage of the dodecamer are shown in Figure 3. The rate constant for the attack at the G-4 deoxyribose, which corresponds to the formation of all products converted to the 3′-phosphorylated trinucleotide [^{32}P]pCGCp following treatment with 1 M piperidine, is at least 1.3 times greater than the rate of scission at any other base.

Not only is the deoxyribose at G-4 the most susceptible to attack by the coordination complex, but the metastable product formed by oxidation at this position also possesses a greater intrinsic stability than the intermediates of other oligonucleotides. Another readily detected metastable band results from the oxidation of the deoxyribose of thymidine-7, yielding a 5′-phosphorylated hexanucleotide product. Although it is not known which structural factors of the DNA helix influence the variable formation or stability of the metastable species, the same cleavage chemistry probably operates at all positions in the sequence. Results with this dodecamer underscore the conclusion that the cleavage chemistry does not depend on any of the structural features of the four bases. Strand scissions corresponding to the oxidation of the deoxyribose at A, T, G, and C all occur in the dodecamer.

The observed first-order rate constant for cleavage in a reaction potentiated by thiol, as calculated from the data in Figure 3B, reflects the lower limit for the chemistry that

involves strand scission. The generation of kinetically significant concentrations of the cuprous complex and hydrogen peroxide must constitute, in part, the rate-limiting step. The addition of 3 mM hydrogen peroxide results in a greater than 2-fold increase in the calculated rate constant of DNA cleavage. The pseudo-first-order rate constant for the formation of the trinucleotide [^{32}P]pCGCp is approximately 10 min^{-1}. Since the rate constant includes the concentration of the coordination complex, estimated at 40 μM (the concentration of added copper ion), the lower limit for the second-order rate constant is 10 $min^{-1}/4.0 \times 10^{-5}$ M or 5×10^3 M^{-1} s^{-1}.

Correlation of Cleavage Sites with Helical Parameters. We searched for correlates between the first-order constants of cleavage at the different sequence positions of the dodecamer and the four parameters of the DNA helix derived from the treatments of Dickerson (1983) and Calladine (1983). These include the helix twist angle, base roll angle, propellor twist, and the torsional angle δ. By use of linear regression analysis with rate constants derived from a single gel lane and helix parameters calculated from the sum function suggested by Dickerson (1983), no statistically significant correlation between any helix parameter and the preferred $(OP)_2Cu^+$ cutting of DNA was found. Similarly, the use of multivariate linear regression methods failed to reveal any statistically significant correlation between combination of helix parameters and the digestion pattern. Replacing the calculated helical parameters with the observed values from the X-ray crystallographic analysis also failed to show any correlations by univariate or multivariate linear regression. The lack of significant correlations suggests that $(OP)_2Cu^+$ does not recognize a single helix parameter as defined above nor a simple linear combination of the four parameters.

Digestion of Netropsin–Dodecamer Complex. The structure of the dodecamer bound to the antibiotic netropsin has also been solved by X-ray crystallographic methods (Kopka et al., 1985a,b). The structural studies reveal that the drug binds to the minor groove of the dodecamer spanning the AATT sequence and displaces a spine of water molecules. Hydrophobic and van der Waals nonbonded contacts between the DNA minor groove atoms and the netropsin pyrroles appear to provide the primary stabilizing interactions between the drug and the DNA. The disruption of these stabilizing interactions by the $-NH_2$ at the C-2 of guanine probably accounts for the specificity of netropsin for A-T-rich regions. Since this structure offers the possibility of correlating the reactivity of the three-dimensional structure with cleavage efficiency, we used the DNA–drug complex as a substrate for the artificial nuclease activity. Moreover, analysis of its reaction with the coordination complex provided an opportunity to assess the reliability of the coordination complex as a footprinting reagent for studying the binding of small organic ligands to DNA.

The strong inhibition of cutting corresponding to the oxidation of the deoxyriboses at C-9, T-8, T-7, and A-6 (Figure 4) constitutes the most striking feature of the digestion pattern of the netropsin–dodecamer complex. This protection provides direct evidence for the attack of the coordination complex from the minor groove. However, it does not differentiate between an intercalative mode of $(OP)_2Cu^+$ binding or a minor groove binding model. Additional features of the digestion pattern help to discriminate between the two models. Although netropsin binds to the tetranucleotide TTAA at positions 8, 7, 6, and 5 within the minor groove, protection of the deoxyribose residues is displaced one nucleotide to the 3′-end. Molecular models indicate that $(OP)_2Cu^+$ can approach the

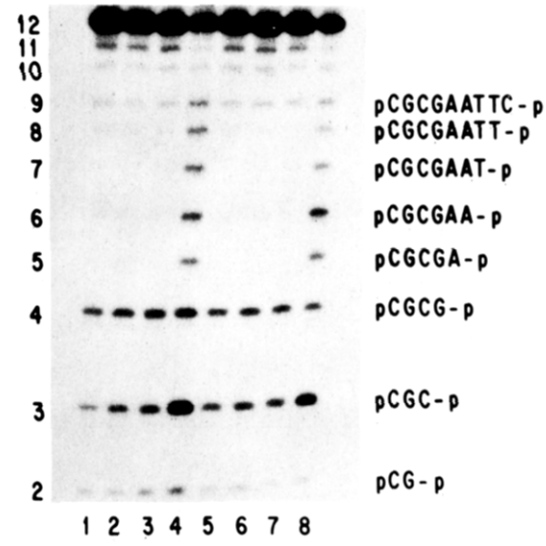

FIGURE 4: Footprinting netropsin–dodecamer complex with $(OP)_2Cu^+$. Netropsin at the indicated concentration was incubated with 0.2 μM ^{32}P-labeled dodecamer and 2 μM of the cold dodecamer for 15 min at 37 °C (lanes 1–4) and 1 h at 0 °C (lanes 5–8) in 50 mM Tris-HCl, pH 8.0. Digestion was carried out with 170 μM OP and 38 μM $CuSO_4$ for 10 min at 37 °C. Prior to being loaded on a sequencing gel, the products were treated with piperidine. Concentration of netropsin (nM): (lane 1) 20; (lane 2) 6; (lane 3) 2; (lane 4) 0; (lane 5) 20; (lane 6) 6; (lane 7) 2; (lane 8) 0.

deoxyribose of adenosine-5, resulting in the production of the tetramer if $(OP)_2Cu^+$ attacks from the minor groove. Intercalative models, which would require a gross distortion of the DNA helix, cannot be similarly rationalized. Furthermore, while the deoxyribose of A-5 suffers oxidative cleavage, the deoxyribose of its complementary base T-8 remains protected from $(OP)_2Cu^+$. This observation is compatible with a minor groove binding intermediate that does not significantly alter the geometry of the DNA.

The loss of the preferential oxidation of the G-4 sugar and the concomitant decrease in the formation of the trinucleotide [^{32}P]pCGCp represents a second noticeable difference in the digestion pattern of the dodecamer–netropsin complex as compared to the digestion of the dodecamer alone. The rate of formation of the trinucleotide equals that of the product formed by the oxidation of adenosine at position 5, a residue that interacts directly with the netropsin. Possibly, the slight widening of the minor groove at T-8 accompanying binding to netropsin is responsible for the relative inhibition of the oxidation of the deoxyribose of G-4. Alternatively, the inhibition of oxidation at G-4 may arise from the efficient trapping of hydroxyl radicals by the proximal guanidinium terminus of netropsin, which extends toward the deoxyribose.

Digestion of EcoRI–Dodecamer Complex. The elegant work of Rosenberg and colleagues on the crystal structure of the *Eco*RI complex with a tridecamer composed of the dodecamer with a thymidylate residue at the 5′-end has provided the first example of a crystal structure of a DNA binding protein or enzyme with its recognition sequence (Frederick et al., 1984). They definitively proved that *Eco*RI recognizes the oligonucleotide by interactions that occur in the major groove. The minor groove remains accessible to solvent. Furthermore, the tridecamer undergoes some deformations including small kinks and helix unwinding but remains as B-form DNA.

$(OP)_2Cu^+$ digestion of the *Eco*RI dodecamer complex provides the strongest evidence for the minor groove attack of $(OP)_2Cu^+$. Comparison of the densitometer traces of the dodecamer cut by the coordination complex in the presence

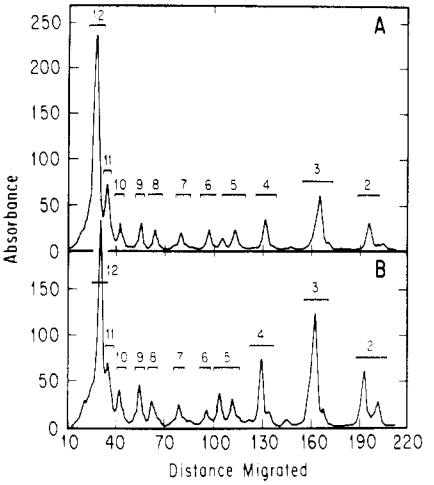

FIGURE 5: Footprinting of *Eco*RI–dodecamer complex with $(OP)_2Cu^+$. *Eco*RI (1.0 μM) was added to 1.0 μM labeled double-stranded dodecamer in 50 mM Tris-HCl, pH 7.5, and 50 mM NaCl and incubated for 15 min at 37 °C. Digestion was carried out at 5 and 10 min with 170 μM OP, 38 μM $CuSO_4$, and 4.8 mM mercaptopropionic acid. (A) Densitometer trace with *Eco*RI after 5 min; (B) control, dodecamer alone.

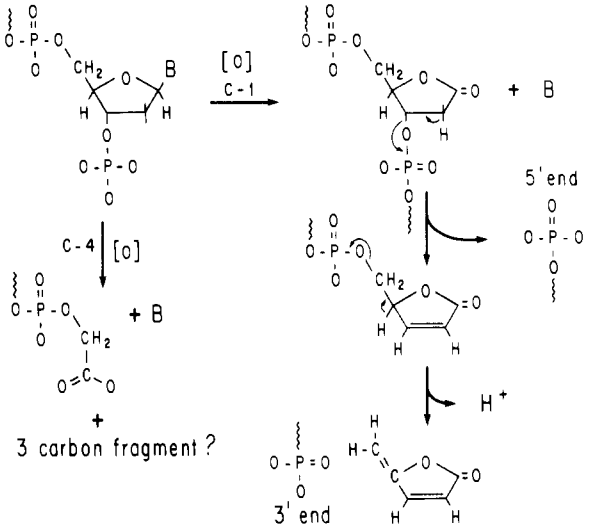

FIGURE 6: Proposed mechanism for scission of DNA by $(OP)_2Cu^+$ and H_2O_2.

and absence of *Eco*RI demonstrates that the binding of the enzyme does not provide any base-specific protection from oxidation by $(OP)_2Cu^+$ (Figure 5). All the deoxyriboses of the dodecamer are accessible to attack. Intercalation of the coordination complex would necessitate large deformations of the DNA that are not possible if the DNA is already bound by *Eco*RI. A minor groove binding mode of attack on the deoxyribose, however, is entirely consistent with the observed cleavage pattern since the structural data indicate that *Eco*RI embraces most of the major groove but leaves the minor groove unprotected. Two controls demonstrate that the magnesium-free apoenzyme binds to the dodecamer. First, it inhibits DNase I cleavage of the dodecamer; second, addition of magnesium ion to the incubation mixture results in precise endonuclease cleavage.

Discussion

The results of the present study permit valuable deductions relevant to the stereochemistry and mechanism of the scission reaction by $(OP)_2Cu^+$. All the data currently available suggest that $(OP)_2Cu^+$ attacks the DNA from the minor groove. This site of interaction of the coordination complex with the DNA had initially been proposed because of a two to three base stagger in the sites of cutting of the two strands of a restriction fragment comprising the *Escherichia coli* tRNA gene (Drew & Travers, 1984). A similar tendency was observed in the cleavage of a restriction fragment containing the *lac* operon control region, but clear exceptions were apparent (Spassky & Sigman, 1985). The three lines of experimental evidence presented here have provided the strongest evidence for the minor groove as the primary site of attack by the synthetic nuclease.

The product analysis is fully consistent with a minor groove reaction mechanism. The formation of all products that have now been identified, including free base, 3′- and 5′-phosphomonoester termini, 3′-phosphoglycolates, and the metastable 3′-intermediate, can be integrated into a reaction scheme (Figure 6). This scheme considers that the oxidative attack from within the minor groove is initiated by hydrogen abstraction from either the C-4 or C-1 positions by the copper–oxo species generated by the one-electron oxidation of the cuprous complex by hydrogen peroxide. The metal-associated hydroxyl radical species could then attack to initiate the two degradative pathways illustrated. This scheme incorporates an important feature of our experimental findings—namely, metastable intermediates are detectable on the 3′-end but not the 5′-end. Although it can account for all the known stable products of the reaction, free bases, and 3′- and 5′-phosphorylated termini, and 3′-phosphoglycolates, it is unproven until the predicted five-carbon fragment of the deoxyribose is isolated.

Recent studies on the mechanism of DNA degradation of bleomycin have demonstrated that a common intermediate formed by hydrogen abstraction at C-4 is responsible for the oxygen-dependent production of 3′-phosphoglycolates and base propenals and for the anaerobic hydrogen peroxide dependent formation of free bases and alkaline-labile sites (Wu et al., 1985a,b). These findings may not be directly applicable to the mechanism of $(OP)_2Cu^+$ degradation because the pathway that forms free bases is associated with phosphodiester bond scission at physiological temperatures and pHs. In addition, the results reported in Figure 1 are not consistent with a single intermediate that partitions into two products. The ratio of 3′-phosphoglycolate to 3′-phosphate is variable and suggestive of different rates of attack at two loci and not the partitioning of a common intermediate. Attack at the hydrogen of C-3, in contrast to that at C-4 or C-1, would imply a major groove attack, which is not consistent with footprinting results obtained with netropsin or *Eco*RI. However, a mechanism for oxidation at C-3 can be written that anticipates the known stable products other than the phosphoglycolates. Since it predicts a different five-carbon fragment than that involving hydrogen abstraction from C-1, the two mechanisms should be distinguishable with further work.

The competitive inhibition of dodecamer cleavage by the antitumor drug netropsin represents a second line of evidence for a minor groove cleavage mechanism. Protection of a unique segment of the dodecamer by netropsin, a drug known to bind selectively to the AT region of the oligonucleotide, strongly implicates the minor groove as the site of interaction with the coordination complex. We can readily interpret the single base pair displacement in the DNA cleavage in terms of the intrinsic geometry of deoxyribose positions in the minor groove. An intercalative model, however, cannot easily explain this shift.

A third line of evidence stems from the $(OP)_2Cu^+$ digestion pattern of the dodecamer bound to *Eco*RI in the absence of

the catalytically essential magnesium ion. The crystallographic analysis of the enzyme–DNA complex reveals significant interaction only in the major groove of the DNA (Frederick et al., 1984). The minor groove remains relatively accessible to solvent and chemical reagents such as $(OP)_2Cu^+$. Binding of the restriction enzyme does not inhibit the rate of cleavage of that region by $(OP)_2Cu^+$. Analysis of the two dodecamer complexes therefore provides complementary evidence for the action of $(OP)_2Cu^+$ as a minor groove specific reactant.

Comparison of the yields of phosphoglycolate termini from ^{60}Co and $(OP)_2Cu^+$ provides insight into the nature of reactive intermediates directly responsible for strand scission. The γ-radiation of ^{60}Co is a hydroxyl radical generator under aerobic conditions. The lack of sequence preference in the cleavage of the dodecamer shown by these radicals suggests that they are freely diffusible. Furthermore, these hydroxyl radicals generate equivalent amounts of 3′-phosphomonoester termini and 3′-phosphoglycolate termini. $(OP)_2Cu^+$ with its essential coreactant hydrogen peroxide is also a hydroxyl radical generator because of the Haber–Weiss chemistry:

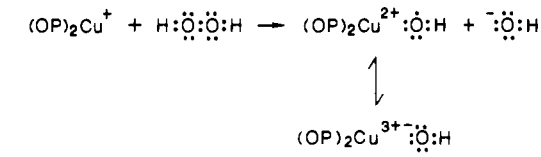

The nuclease activity of $(OP)_2Cu^+$ and hydrogen peroxide exhibits a sequence-dependent variability of phosphoglycolate production. At the same base position, the yield of phosphoglycolate is usually less than the yield of 3′-phosphomonoester. The coordination complex, therefore, is not generating hydroxyl radicals that are as diffusible as the hydroxyl radical produced by γ-radiation. The hydroxyl radical produced from the coordination complex must either remain associated with the copper or, if it is released, be directed away from the C-4-hydrogen in order to diminish the yields of 3′-phosphoglycolates, which presumably form as a result of attack at this position. The observed sequence-dependent variability in 3′-phosphoglycolate products implies that conformational differences in the minor groove serve to orient the hydroxyl radical before its attack on the deoxyribose. The reduced yield of phosphoglycolate distinguishes $(OP)_2Cu^+$ not only from ^{60}Co-generated hydroxyl radical chemistry but also from the reaction with methidiumpropyl-EDTA–Fe(II) (Van Dyke & Dervan, 1984). This oxidative nucleolytic activity gives a product distribution similar to that observed with ^{60}Co-potentiated cleavage. Minor groove attack by $(OP)_2Cu^+$ has previously been suggested on the basis of the assumption that the coordination complex generated diffusible hydroxyl radicals that could nick both strands equivalently (Drew, 1984; Drew & Travers, 1984). Although the suggestion for minor groove attack appears to be valid, the experiments presented in this paper provide the strongest evidence for it.

In summary, the artificial nuclease activity of $(OP)_2Cu^+$ accomplishes strand scission by oxidatively degrading the deoxyribose from within the minor groove. Scission takes place at all four bases because no specific feature of a base's structure is required either for the binding of $(OP)_2Cu^+$ or for the chemistry of the cleavage. The experiments reported here strongly imply that the coordination complex attacks from within the minor groove. The reagent therefore may provide a method for determining if a ligand binds within the minor groove. It can also identify sequence-dependent variation of minor groove structure in DNA and permit its correlation with biological function.

ACKNOWLEDGMENTS

We are grateful for helpful comments by Dr. Betty Chen, Dr. Mary Kopka, and Professor Richard Dickerson. Professor D. Rees made valuable suggestions for the analysis of kinetic data; Professor J. Rosenberg generously provided a gift of magnesium-free *Eco*RI.

Registry No. $(OP)_2Cu^+$, 17378-82-4; 5′-CGCGAATTCGCG-3′, 77889-82-8; DNase, 9003-98-9; H_2O_2, 7722-84-1.

REFERENCES

Burger, R., Berkowitz, A. R., Peisach, J., & Horwitz, S. B. (1980) *J. Biol. Chem. 255*, 11832–11838.

Calladine, C. R. (1982) *J. Mol. Biol. 161*, 343–352.

Cartwright, I. L., & Elgin, S. C. R. (1982) *Nucleic Acids Res. 10*, 5835–5852.

Dickerson, R. E. (1983) *J. Mol. Biol. 166*, 419–441.

Dickerson, R. E., & Drew, H. R. (1981a) *J. Mol. Biol. 149*, 761–786.

Dickerson, R. E., & Drew, H. R. (1981b) *Proc. Natl. Acad. Sci. U.S.A. 78*, 7318–7322.

Dickerson, R. E., Drew, H. R., Conner, B. N., Wing, R. M., Fratini, A. V., & Kopka, M. L. (1982) *Science (Washington, D.C.) 216*, 475–485.

Drew, H. (1984) *J. Mol. Biol. 176*, 535–557.

Drew, H. R., & Dickerson, R. E. (1981a) *J. Mol. Biol. 151*, 535–556.

Drew, H. R., & Dickerson, R. E. (1981b) *J. Mol. Biol. 152*, 723–736.

Drew, H. R., & Travers, A. (1984) *Cell (Cambridge, Mass.) 37*, 491–502.

Fratini, A. V., Kopka, M. L., Drew, H. R., & Dickerson, R. E. (1982) *J. Biol. Chem. 257*, 14686–14707.

Frederick, C. A., Grable, J., Melia, M., Samudzi, C., Jen-Jacobsen, L., & Wang, B.-C., Greene, P., Boyer, H. W., & Rosenberg, J. M. (1984) *Nature (London) 309*, 327–331.

Henner, W. D., Grunberg, S. M., & Haseltine, W. A. (1982) *J. Biol. Chem. 257*, 11750–1154.

Henner, W. D., Rodriguez, L. O., Hecht, S. M., & Haseltine, W. A. (1983) *J. Biol. Chem. 258*, 711–713.

Hertzberg, R. P., & Dervan, P. B. (1984) *Biochemistry 23*, 3934–3945.

Jessee, B., Garguiulo, G., Razvi, F., & Worcel, A. (1982) *Nucleic Acids Res. 10*, 5823–5834.

Kopka, M. L., Yoon, C., Goodsell, D., Pjura, P., & Dickerson, R. E. (1985a) *J. Mol. Biol. 183*, 553–563.

Kopka, M. L., Yoon, C., Goodsell, D., Pjura, P., & Dickerson, R. E. (1985b) *Proc. Natl. Acad. Sci. U.S.A. 82*, 1376–1380.

Lomonosoff, G. P., Butler, P. J. G., & Klug, A. (1981) *J. Mol. Biol. 149*, 745–760.

Maniatis, T., Fritsch, E. F., & Sambrook, J. (1982) *Molecular Cloning: A Laboratory Manual*, Cold Spring Harbor Laboratory, Cold Spring Harbor, NY.

Marshall, L. E., Graham, D. R., Reich, K. A., & Sigman, D. S. (1981) *Biochemistry 20*, 244–250.

Maxam, A., & Gilbert, W. (1980) *Methods Enzymol. 65*, 499–559.

Patel, D. J., Kozlowski, S. A., Marky, L. A., Broka, C., Rice, J. A., Itakura, K., & Breslauer, K. J. (1982) *Biochemistry 21*, 428–436.

Pope, L. E., & Sigman, D. S. (1984) *Proc. Natl. Acad. Sci. U.S.A. 81*, 3–7.

Pope, L. E., Reich, K. A., Graham, D. R., & Sigman, D. S. (1982) *J. Biol. Chem. 257*, 12121–12128.

Pribnow, D. (1975) *Proc. Natl. Acad. Sci. U.S.A. 72*, 784–788.

Sigman, D. S., Graham, D. R., D'Aurora, V., & Stern, A. M. (1979) *J. Biol. Chem. 254*, 12269–12272.

Sigman, D. S., Spassky, A., Rimsky, S., & Buc, H. (1985) *Biopolymers 24*, 183-197.
Spassky, A., & Sigman, D. S. (1985) *Biochemistry 24*, 8050-8056.
Wu, J. C., Stubbe, J. A., & Kozarich, J. W. (1985a) *Biochemistry 24*, 7562-7568.
Wu, J. C., Stubbe, J. A., & Kozarich, J. W. (1985b) *Biochemistry 24*, 7569-7573.

Molecular Recognition between Oligopeptides and Nucleic Acids: Novel Imidazole-Containing Oligopeptides Related to Netropsin That Exhibit Altered DNA Sequence Specificity†

J. William Lown,* Krzysztof Krowicki, and U. Ganapathi Bhat
Department of Chemistry, University of Alberta, Edmonton, Alberta, Canada T6G 2G2
Andrew Skorobogaty
Department of Biochemistry, La Trobe University, Bundoora, Victoria, Australia 3083
Brian Ward and James C. Dabrowiak
Department of Chemistry, Syracuse University, Syracuse, New York 13120
Received March 27, 1986; Revised Manuscript Received July 29, 1986

ABSTRACT: Oligopeptides have been synthesized that are structurally related to the antiviral antitumor antibiotic netropsin, but in which each of the pyrrole units is successively replaced by an imidazole moiety, as well as their di- and triimidazole-containing counterparts. These compounds bind to duplex DNA with constants in the range (1.06–1.98) × 10^6 M^{-1} but not to single-stranded DNA. Since they bind to T4 DNA, it is inferred that, like the parent antibiotic netropsin, they are also minor groove selective. This series of compounds exhibits a progressively decreasing preference for AT sites in binding studies with both native DNAs and synthetic oligonucleotides and a corresponding increasing acceptance of GC base pairs. Footprinting experiments utilizing a 139 base pair *Hin*dIII/*Nci*I restriction fragment from pBR 322 DNA revealed that these lexitropsins, or information-reading oligopeptides, recognize more sites than the parent netropsin. In addition, some regions of enhanced nuclease action as the result of drug binding to the fragment were identified. The diimidazole compound in particular recognizes GC-rich sites, implying the formation of new hydrogen bonds between G-C(2)NH_2 in the minor groove and the additional N_3 imidazole nitrogens. It is clear however that, since the lexitropsins appear to tolerate the original $(AT)_4$ site, an *N*-methylimidazole group on the ligand will permit either a GC or AT base pair in the binding sequence. Another factor that may be significant in molecular recognition is the high negative electrostatic potential of A·T regions of the minor groove, which is likely to strongly influence binding of these cationic species to DNA. This approach may ultimately permit the structurally rational alteration of sequence specificity in the molecular recognition of oligopeptides for DNA.

The mechanisms whereby peptides, small proteins, and other molecules recognize nucleic acids are fundamental to many important processes in biology and appear to underlie their characteristic properties in living systems (Caruthers, 1980; Ofengand, 1979; Kim et al., 1974; Gursky et al., 1977; Takeda et al., 1983; Frederick et al., 1984). This applies, for example, to DNA–histone interactions (Kim et al., 1974; Gursky et al., 1977), the recognition between enzymes or regulatory proteins and complementary DNA binding sites (Caruthers, 1980; Ofengand, 1979; Kim et al., 1974), and several cases of current clinical interest in anticancer (Neidle & Waring, 1983) and antiviral (Gale et al., 1981) chemotherapy. The binding of such antineoplastic agents as doxorubicin, daunorubicin (Neidle & Waring, 1983; Gale et al., 1981), bleomycin (Hecht, 1979), or neocarzinostatin (Kappen & Goldbert, 1983) to cell target DNA invokes intimate, precise, and highly specific interactions in molecular recognition.

There is increasing knowledge from the molecular biology of gene expression and control, DNA structure and topology, and the recognition of sequences of unusual susceptibility or sensitivity to xenobiotics (Ruddon, 1981). This new information combined with a greater appreciation of structure–activity relationships of anticancer drugs (Neidle & Waring, 1983; Gale et al., 1981) increases the prospects for rational anticancer drug design. Thus, significant advantages would accrue in, for example, the understanding of the processes of gene expression, or the design of vectors for drug targeting, if one could decipher the code controlling the reading of information on DNA by drug molecules. In this regard, a specific goal of ours is to design binding groups to act as vectors for our hemin-based functional bleomycin models (Lown et

†This investigation was supported by grants (to J.W.L.) from the National Cancer Institute of Canada and the Natural Sciences and Engineering Council of Canada and Grant GM 31895 (to J.C.D.) from the National Institutes of Health.

0006-2960/86/0425-7408$01.50/0